

Nano-Engineering of Molecular Interactions in Organic Electro-Optic Materials

Stephanie J. Benight, Bruce H. Robinson and Larry R. Dalton
*University of Washington,
USA*

1. Introduction

Integration of electronic and photonic devices, especially chip-scale integration, is dramatically impacting telecommunication, computing, and sensing technologies (Dalton et al., 2010; Dalton & Benight, 2011; Benight et al., 2009). For organic electronics and photonics, control of molecular order is crucial for effective device performance. For organic photonics, formation of molecular aggregates can result in unacceptable optical loss. For organic electronics, molecular aggregates can adversely influence charge mobilities. Control of intermolecular electrostatic interactions can be exploited to control molecular organization including molecular orientation. Such control can lead to optimized material homogeneity and optical transparency and also to control of molecular conductivity. Here we focus on techniques for systematically nano-engineering desired intermolecular electrostatic interactions into organic electroactive materials. While our primary focus will be on electro-optic materials (which require acentric molecular organization), the discussion is also relevant to optimizing the performance of photorefractive, electronic, photovoltaic, and opto-electronic materials.

Molecular order is known to play a pivotal role in defining bulk material processes specific to electronics and photonics (i.e. photovoltaics, electronics, light-emitting devices and electro-optics) through impact on processes such as charge mobility, nonlinear optical processes, exciton diffusion, etc. A challenge common to electronics and photonics is to develop a fundamental understanding of how intermolecular interactions introduced into functional materials can be used to influence long-range molecular order.

1.1 Organic Electro-Optic (OEO) materials

Organic electro-optic (OEO) materials have the potential to be critical components for next generation computing, telecommunication, and sensing technologies (Dalton et al., 2010). Applications of OEO materials extend to the military and medical sectors where super lightweight aircrafts and non-invasive, powerful imaging are applications of great utility. OEO materials afford the potential for great size, weight, and power efficiency as well as greater bandwidth, lower drive voltages, and greater flexibility in manufacturing and integration (Benight et al., 2009).

OEO molecules or “chromophores” are comprised of conjugated π -electrons that make up their core chemical structure. In the presence of time-varying electric fields, OEO

chromophores exhibit ultrafast charge displacements (on the order of tens of femtoseconds) (Munn & Ironside, 1993). The response time is the phase relaxation time of the π -electron correlation. These response times are superior to that of conventional inorganic crystals (e.g. lithium niobate) typically used widespread in commercial applications; the response time of lithium niobate is defined by ion displacement and is on the order of picoseconds. Of course, other factors such as velocity mismatch of electrical and optical waves and the electrical conductivity of metal electrodes can also influence the bandwidth performance of practical devices (Dalton & Benight, 2011). OEO materials also offer other advantages including the potential for significantly higher EO activity, lower dielectric constants, and amenability to a plethora of techniques including, but not limited to crystal growth, sequential synthesis/self-assembly layer-by-layer growth, deposition from either solution or the gas phase, soft and nano-imprint lithography and gray scale and photolithography, etc. (Kwon et al., 2010; Frattarelli et al., 2009; Dalton et al., 2010).

Several different types of OEO materials have been developed in previous research, some of which have been implemented into viable photonic device structures (Shi et al., 2000; Blanchard-Desce et al., 1999; Sullivan et al., 2007). One of the most prevalent types of OEO systems involves a strongly dipolar ellipsoidal-shaped molecule comprised of an electron donor, π -conjugated bridge, and electron acceptor units; this type of molecule is typically denoted as a “push-pull” chromophore. Because they are comprised of electron donor, bridge, acceptor, OEO chromophores tend to have large dipole moments which translate to exhibiting strong dipole-dipole anti-parallel pairing intermolecular interactions (lowest energy configuration) in a bulk system. Fig. 1 illustrates an example of an OEO push-pull chromophore (A) and a cartoon illustrating bulk anti-parallel dipole-dipole pairing (B).

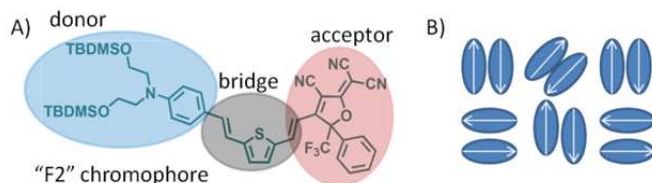


Fig. 1. A) Example of a push-pull organic electro-optic chromophore with the donor, bridge, and acceptor units highlighted. B) Cartoon illustrating dipole-dipole anti-parallel pairing with the blue ellipsoids representing chromophores and the arrows representing dipoles

In addition to dipolar chromophores, other types of chromophores such as octupolar have been explored (Blanchard-Desce et al., 1999; Valore et al., 2010; Ray & Leszczynski, 2004). Unfortunately, such chromophores have yet to be implemented into device structures. The reader is referred elsewhere for more information on these types of EO materials as our discussion here will focus on dipolar rod-shaped chromophores and systems based from these types of molecules (Dalton et al., 2011).

Before proceeding further, it is important to discuss the basis for the bulk properties of OEO materials. The EO activity of materials originates from the nonlinear susceptibility or macroscopic polarization response of a material, given in Eq. 1.

$$\mathbf{P}_i = P_0 + \chi_{ij}^{(1)} \mathbf{E}_j + \chi_{ijk}^{(2)} \mathbf{E}_j \mathbf{E}_k + \chi_{ijkl}^{(3)} \mathbf{E}_j \mathbf{E}_k \mathbf{E}_l \dots \quad (1)$$

Certain materials express higher ordered moments of susceptibility when exposed to high intensity electromagnetic radiation. In the equation above, $\mathbf{P}_i = P_0 + \chi_{ij}^{(1)}$, is the first order (linear) polarizability, $\chi_{ijk}^{(2)}$ is second order and $\chi_{ijkl}^{(3)}$ is third order, etc.

Several physical processes can be expressed within the higher ordered moment terms (second order, third order, etc.) of the macroscopic polarization, but materials must exhibit certain properties or behavior to do so. For example, the basis for EO activity is the Pockels Effect, which is a second order nonlinear process inherent in the second ordered term, $\chi_{ijk}^{(2)}\mathbf{E}_j\mathbf{E}_k$ in Eq. 1. The Pockels effect is expressed when a change in the refractive index (birefringence) is induced in the material as caused by a constant or varying electric field (Munn & Ironside, 1993; Sun & Dalton, 2008).

In order for the Pockels effect or any other even ordered process to be expressed, the material must be noncentrosymmetric (bulk acentric order). In addition to a macroscopic response, a microscopic polarization response must also be demonstrated on a molecular basis. The microscopic nonlinear polarization, p_i , is represented as

$$p_i = p_0 + \alpha_{ij}^{(1)}\mathbf{E}_j + \beta_{ijk}^{(2)}\mathbf{E}_j\mathbf{E}_k + \gamma_{ijkl}^{(3)}\mathbf{E}_j\mathbf{E}_k\mathbf{E}_l \dots \quad (2)$$

The terms α , β , γ , etc. in the equation are second, third, and fourth rank tensors, respectively. The term, $\beta_{ijk}^{(2)}\mathbf{E}_j\mathbf{E}_k$, is the second order polarization response and $\beta_{ijk}^{(2)}$ is the molecular first hyperpolarizability for an individual chromophore molecule. The component of the tensor along the dipolar axis of the chromophore is denoted as β_{zzz} . Within these tensor elements lies three interrelated components: (1) vector components of the molecular electronic density distribution, (2) direction and polarization of light that is propagating through the material and (3) the direction and polarization of externally low-frequency applied fields. Optimizing β has a direct impact on the macroscopic NLO second order susceptibility, $\chi^{(2)}$ through the relationship expressed in Eq. 3.

$$\chi_{zzz}^{(2)}(\omega) = N\beta_{zzz}(\omega, \varepsilon)\langle \cos^3 \theta \rangle g(\omega) \quad (3)$$

where $\chi_{zzz}^{(2)}$ is dependent on the frequency (ω) of the incident light; N is the number density of the material or the concentration of chromophores in the material system; $\beta_{zzz}(\omega, \varepsilon)$ is dependent on both frequency and material dielectric; $\langle \cos^3 \theta \rangle$ is the acentric order parameter in the material or the orientational average of the angle (θ) between the z (dipolar) axis of a chromophore and the z direction of the externally applied electric field; and $g(\omega)$ represent effects of local fields upon the chromophore molecules.

The EO coefficient, r_{33} , is the principal tensor element of the linear EO coefficient, \mathbf{r}_{ijk} . Short for r_{333} , r_{33} is the tensor element that corresponds to the polarization of the optical beam and the direction of the externally applied electrical field both in the z direction. $\chi_{zzz}^{(2)}$ is related to r_{33} through Eq. 4 (Munn & Ironside, 1993).

$$\frac{2\chi_{zzz}^{(2)}(\omega)}{n^4} = r_{33}(\omega) \quad (4)$$

where n in the material refractive index.

Eq. 4 demonstrates that r_{33} can be improved by targeting improvement of three parameters, $\beta_{zzz}(\omega, \varepsilon)$, N , and $\langle \cos^3 \theta \rangle$ as illustrated in Eq. 5.

$$r_{33} \propto N\beta\langle \cos^3 \theta \rangle \quad (5)$$

Research efforts in the past have focused on improving one or more of these parameters through molecular and material system design. In order to further understand the nano-engineering approach described herein, a brief history of EO systems development will be discussed.

1.2 Past approaches in improving EO activity

Many past efforts have had the goal of designing chromophores with superior hyperpolarizability, β_{zzz} . Early EO materials consisted of a chromophore as a guest in a host amorphous polymer system (Zhang et al., 2001). The most sophisticated, best-performing chromophores with the largest hyperpolarizabilities are those that contain a heteroaromatic or polyene (isophorone-protected) bridge in the chromophore core structure. An example of both of these types of chromophores is given in Fig. 2.

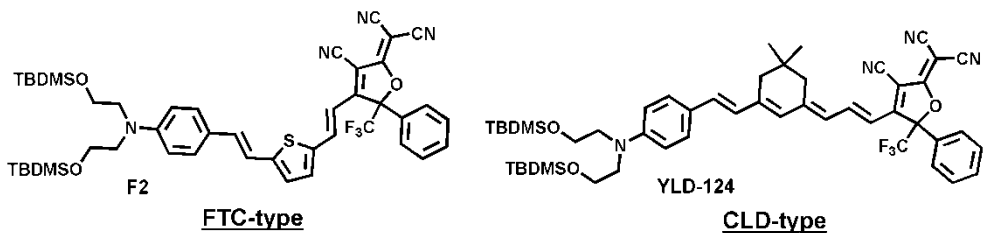


Fig. 2. Example structures of FTC-type and CLD-type chromophores are given with a heteroaromatic bridge and isophorone bridge as identifiers. The specific names for these structures, F2 and YLD-124, are also given beneath each structure. "F2" is given as a name of the structure for ease of reference and "YLD-124" is named after the inventor of the compound

Chromophores of this nature, known as FTC-type and CLD-type, respectively, are the basis for OEO chromophores used in the limited number of commercial devices today and in ongoing research for implementing OEO materials into silicon hybrid inorganic device structures (Baehr-Jones et al., 2008; Ding et al., 2010; Michalak et al., 2006). "FTC" is an abbreviation that stands for "furan-thiophene chromophore" since the chemical structure contains these moieties; "CLD" is named after the authors who first introduced the molecular structure (Zhang et al., 2001). Such acronyms are widely referred to in specialized literature and we include them here for ease of reference. While many other improvements have been made in exploring various chromophore donors, bridges, and acceptors (Davies et al., 2008; Cheng et al., 2007; Cheng et al., 2008), these two base structures are the best in terms of hyperpolarizability, performance, ease of synthesis, and low absorption at the telecommunications (applications) wavelengths.

However, in examining Eq. 5, we see that r_{33} also depends on the number density or the concentration of chromophores in the system. Because of the strong intermolecular dipole-dipole antiparallel pairing interactions, such guest-host systems are often limited to number densities of ~20 % (Benight et. al., 2010). As was discussed earlier, chromophores possessing large hyperpolarizabilities also possess large dipole moments (on the order of 25 Debye), making designing chromophore with larger hyperpolarizabilities problematic. Additionally, in order to have an appreciable electro-optic effect (a second order nonlinear process), these molecules must exhibit noncentrosymmetry (be ordered in an acentric manner (i.e. uniformly or in one direction)). With increasing concentration of chromophores in the system, dipole-dipole pairing increases which negates any acentric order ($\langle \cos^3\theta \rangle$) in the system. Such dipole-dipole intermolecular pairing also causes aggregation of chromophores at high number densities, leading to undesired optical loss and conductivity at poling temperatures.

To prevent or limit dipole-dipole intermolecular pairing in bulk systems containing EO chromophores, bulky groups have been synthetically attached to chromophores to inhibit close approach. This method of "site (chromophore)-isolation" has been shown to limit chromophore aggregation (Liao et. al., 2005; Hammond et. al., 2008; Kim et. al., 2008). In this approach, bulky groups such as dendrons are covalently attached the chromophore core, therefore prohibiting one chromophore molecule from getting too close spatially to another chromophore molecule. In addition, multi-arm EO chromophore dendrimers have also been designed and synthesized and shown to permit high number densities of chromophores to be achieved without unwanted effects (Sullivan et. al., 2007).

Another approach that has been utilized and has yielded high EO activities on the order of 300 pm/V is preparation of binary chromophore organic glasses (BCOGs) (Kim et. al., 2006, 2008; Sullivan et. al., 2007). BCOGs are prepared by mixing chromophore guest molecules into chromophore-containing host molecules. Such systems can tolerate chromophore concentrations on the order of 60%. Both guest and host molecules are polar, resulting in favorable entropy of mixing and an absence of solvatochromic shifts with changing chromophore compositions. A dimensional restriction is also imposed because less freedom for movement of guest chromophores is able to be achieved, contributing to higher chromophore order and also higher EO activity (Benight et. al., 2010).

1.3 Improving EO activity through increased acentric order

With the success of site-isolation and BCOG approaches, improvement of acentric order by chromophore modification, such as incorporation of additional and specific intermolecular electrostatic interactions, has remained a less pursued goal. Realization of molecular and supramolecular architectures with desired long-range acentric order in glassy materials remains a fundamental challenge.

1.3.1 Electric field poling

Most as-synthesized OEO materials are disordered, i.e. $\langle \cos^3\theta \rangle$ and $r_{33} = 0$. The most commonly employed method for inducing acentric order into a chromophore system is to apply an electric field in the z direction (perpendicular to a device substrate) while heating the material to near its glass transition temperature. This electric field poling is the primary

method utilized to induce acentric order into conventional poled guest-host polymer composites, EO dendrimers, and BCOG systems (Dalton et. al., 2010). For chromophore-polymer composites using solely electric field poling, the highest acentric order that is commonly achieved is on the order of 0.05 or lower (Benight et. al., 2010).

1.3.2 Other acentric ordering approaches

Approaches other than electric field poling that have also been explored have mainly consisted either of sequential synthesis of self-assembling chromophore systems or growing noncentrosymmetric crystal lattices of OEO chromophores (Kang et. al., 2004; Facchetti et. al., 2004; van der boom et. al., 2001; Frattarelli et. al., 2009; Kwon et. al., 2010). In addition and more recently, chromophores capable of being vapor deposited onto a substrate while undergoing electric field or laser-assisted electric field poling have demonstrated high acentric order (Wang et. al., 2011).

Self assembly approaches that have been successful to the present have utilized chromophores with modest β values. These chromophores are deposited through solution or vapor-phase self assembly with a functionalized monolayer tethered to the surface of the substrate. Marks and coworkers have demonstrated this concept for both OEO materials and materials in Organic Field Effect Transistors (OFETs) (Kang et. al., 2004; Facchetti et. al., 2004; van der boom et. al., 2001; Frattarelli et. al., 2009; DiBenedetto et. al., 2008). Recently, another self assembly approach has involved utilizing chromophores with weak hyperpolarizabilities and vapor depositing them on a surface under the influence of a polarized optical (laser) field as well as an electric poling field (Wang et. al., 2011). In this approach utilized by Chen and coworkers, the chromophore BNA (Benzyl-2-methyl-4-nitroaniline) has achieved r_{33} values ~ 40 pm/V with an acentric order parameter nearly unity. This approach is referred to as Laser-Assisted Poling - Matrix Assisted Poling (LAP-MAP) because the intermolecular BNA-BNA crystal forming interactions juxtaposed with the assistance of the poling field orient the chromophores in the material matrix. Albeit, BNA has been demonstrated to grow into noncentrosymmetric crystals without the presence of a poling field, laser-assisted electric field poling permits the acentric order to be achieved in a direction appropriate for waveguide device structures (Wang et. al., 2011).

Even though systems have been demonstrated in which chromophores exhibit higher acentric order as a result of self-assembly mechanisms, such systems have not utilized chromophores with large hyperpolarizabilities (β) and their fabrication methodologies are not easily adapted to chromophores with large β . High order does not adequately compensate for lower β and lower r_{33} values are the result. Moreover, defects propagate in sequential synthesis/self-assembly methods and thus film thicknesses are typically limited to 150 nm or less.

An alternative route to achieving acentric order in EO materials has been to grow noncentrosymmetric crystals of chromophore molecules (Kwon et. al., 2010; Yang et. al., 2007; Hunziker et. al., 2008; Weder et. al., 1997). A handful of EO chromophores when grown from a melt are able to crystallize in a noncentrosymmetric crystal lattice. Examples of such molecules are shown in Fig. 3.

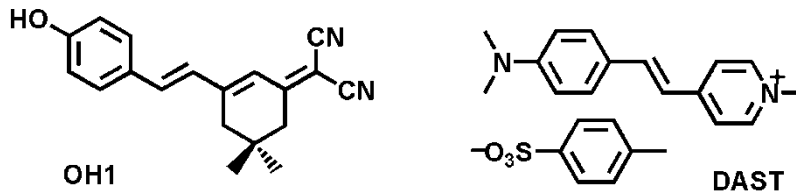


Fig. 3. The crystal growth chromophores, OH1 and DAST, shown

These chromophores, possessing low hyperpolarizabilities, yield acentric order parameters of $\langle \cos^3\theta \rangle$ between 0.7-0.9 and EO activities of $r_{33} = 52$ pm/V at 1313 nm for OH1 and $r_{11} = 53$ pm/V at 1319 nm for DAST (Rainbow Photonics, 2011). However, designing chromophores that will crystallize into a noncentrosymmetric crystal is unpredictable and extremely sensitive to small structural details. For example, in attempting to improve the chromophore structure of OH1, changing chirality of one bond, extending a bond by one additional carbon, or any slight alteration in chemical structure can result in a centrosymmetric rather than a noncentrosymmetric crystal. This unpredictability makes chromophore design and improvement quite difficult and left to synthetic trial and error. It is possible that such crystal formations may be able to be modeled using theoretical methods, but such guidance is not yet available. In addition, it can be difficult and time-consuming to achieve such crystals, taking away from the efficacy in efficient processing of organic EO chromophores. Another disadvantage of crystal growth methods is the potential for light scattering from crystalline micro-domain formation.

1.3.3 Nano-engineering of directed interactions for increased acentric order

As already mentioned, the primary method for inducing acentric order is electric field poling. Recently, efforts to improve poling-induced order have involved incorporation of additional and specific intermolecular electrostatic interactions into synthesized chromophores. Dalton and Jen have employed covalent attachment of directed molecular interactions to enhance the poling-induced acentric order (Dalton et. al., 2011). Interactions such as arene-perfluorarene (Ar-pFAR) and coumarin-coumarin have yielded some of the highest EO activities to date, ranging from 140-450 pm/V (Kim et. al., 2007, 2008; Zhou et. al., 2009; Benight et. al., 2010). Such systems embody covalent attachment of pendant groups, which interact with each other, to the chromophore cores of the molecules. In the case of Ar-pFAR interactions, an arene group is covalently attached to the chromophore donor substituent while a pFAR group is attached to the bridge substituent of the chromophore. In a bulk system the Ar and pFAR pendant groups intermolecularly interact (via quadrupolar interaction), exhibiting a self-assembly-like behavior. In the presence of an electric poling field, these pendant groups help to assist the acentric ordering of the chromophore molecules (Benight et. al., 2010; Dalton et. al., 2011; Dalton & Benight, 2011).

In addition to Ar-pFAR interactions, coumarin-based pendant groups can also be covalently attached to different portions of the chromophore core. In this case, Benight and coworkers have synthesized a series of compounds in which two coumarin-containing pendant groups are attached to the chromophore core of the molecule. Specifically, an alkoxybenzoyl-coumarin with a 6 carbon chain linker was covalently attached the chromophore core at both the donor and bridge portions to make the prototype molecule "C1" (Benight et. al., 2010). Through

extensive characterization, to be recounted later in this Chapter, it was shown that the coumarin groups interact intermolecularly to restrict the rotational movement or lattice dimensionality of the chromophore cores in the bulk system. Lattice dimensionality can be further explained using theoretical methods (see Section 2.6) such as Monte Carlo theoretical modeling (see Section 2.7). As a result, the material system exhibits higher centrosymmetric and acentric order, yielding significantly enhanced EO activities. Experimental methods also demonstrate that coumarin-coumarin interactions lead to long range molecular cooperativity and that the coumarin moieties are oriented in a plane orthogonal to the poling-induced order of the chromophores (Benight, 2011; Benight et. al., 2011). These experimental results are also corroborated by molecular dynamics theoretical methods. This lattice dimensionality restriction and resulting improvement in poling-induced order is referred to as Matrix Assisted Poling (MAP). This approach can be expanded to include covalently attaching pendant groups which are molecules that differ in structure and property from the EO material and that organize in type of intermolecular interaction unique from that of the EO material (Benight et. al., 2010). Such spatially anisotropic interactions include but are not limited to dipolar, quadrupolar, and ionic interactions.

Herein, this nano-engineering of chromophores will be described in detail with an overview and explanation of the behavior of C1 through a developed toolset of comprehensive experimental characterization and theoretical methods. Instrumental methods are of the utmost importance to detect and probe pendant group molecular interactions, chromophore-chromophore interactions, and acentric/centric order of the molecular system. Several experimental methods are of great utility including optical ellipsometric methods, methods for characterizing electro-optic activity (e.g., attenuated total reflection, ATR), and methods for measuring viscoelastic behavior. Specific methods to be discussed include Attenuated Total Reflection (ATR) (Chen et. al., 1997), Variable Angle Polarization Referenced Absorption Spectroscopy (VAPRAS) (Olbricht et. al., 2011), Variable Angle Spectroscopic Ellipsometry (VASE) (Woollam, 2000), Shear-Modulation Force Microscopy (SM-FM) (Ge et. al., 2011), Intrinsic Friction Analysis (IFA) (Knorr et. al., 2009a), and Dielectric Relaxation Spectroscopy (DRS) (Dalton et. al., 2011). These methods provide complementary and synergistic understanding of the roles played by various intermolecular electrostatic interactions. Furthermore, theoretical methods such as rigid body Monte Carlo (RBMC) methods and coarse-grained Molecular Dynamics (MD) simulations are invaluable and will also be discussed

2. Recent results and discussion of nano-engineered OEO chromophore systems

2.1 The preparation of C1

The strategy of nano-engineering intermolecular interactions into organic functional materials systems involves a three pronged approach of synthesis, characterization, and theoretical simulation. As an example, we focus on the C1 molecule involving coumarin attachment to an FTC-type chromophore core. The C1 chemical structure is shown in Fig. 4. Alkoxybenzoyl-coumarins were attached to the donor and bridge portions of an EO (FTC-type) chromophore with large hyperpolarizability. The alkoxybenzoyl-coumarin pendant groups in C1 have been shown to exhibit highly planar liquid crystalline thermotropic phases (Tian et. al., 2003, 2004).

The approach in the design of C1 was to use the intermolecular interactions amongst coumarin molecules that govern liquid crystal phase formation to assist in the unidirectional (acentric) ordering of the highly dipolar chromophores in an electric field. As explained above, being able to mitigate intermolecular interactions in the EO material system is important in order to be able to induce and sustain acentric order and therefore, appreciable EO activity (r_{33}). The effect of coumarins can be interpreted as improvement of EO activity by reduction of effective lattice symmetry in the vicinity of the EO chromophore (Benight et. al., 2010).

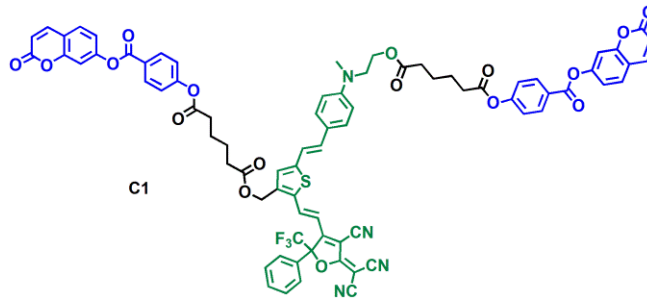


Fig. 4. The structure of C1 is shown with the EO active chromophore unit highlighted in green and the alkoxybenzoyl coumarin units highlighted in blue

C1 was synthesized in a multi-step (15 total steps) synthesis (Benight et. al, 2011; Benight, 2011). First, the chromophore core comprised of donor and bridge components was prepared according to procedures established in the literature (Sullivan et. al., 2007). The chromophore was modified to have two ethoxy groups to act as points of pendant group attachment on both the donor and bridge of the chromophore. In parallel, the coumarin pendant group was prepared through a 4-step synthesis involving a series of modified Steglich esterifications by first preparing the pendant group itself (coumarin-containing mesogen) followed by attaching an adipic acid linker to act as the connection point between chromophore and pendant group. Once the chromophore core (all components minus acceptor) and the pendant group was prepared, the pendant group was then attached to the chromophore through an esterification reaction. The final step in the synthesis of C1 was attaching the electron acceptor (also prepared separately according to a literature procedure) via a Knoevenagel condensation (Liu et. al., 2003).

2.2 EO activity of C1

To evaluate physical properties including EO activity, samples of C1 were spin coated from organic solvent into thin films on ITO coated substrates and titanium dioxide (TiO₂) coated ITO substrates. TiO₂ has been shown to be quite useful as a blocking layer in organic materials-based devices by acting as a Schottky-type barrier in blocking excess charge injection into the organic layer (Sprave et. al, 2006; Enami et. al., 2007; Huang et. al., 2010). We have found this is to be the case in our EO characterization experiments both in poling more conventional poled polymer materials as well as MAP systems like C1, achieving upwards of 30% more effective electric field poling and EO activities. r_{33} values for C1 were acquired using the widely applied technique of attenuated total reflection (ATR). The use of

ATR for characterization of EO materials is described in detail elsewhere (Benight, 2011; Davies et. al., 2008; Herminghaus et. al., 1991; Chen et. al., 1997). Although several methods for characterizing EO coefficients exist, most notably Teng-Man Simple Reflection Ellipsometry (Teng & Man, 1990; Park et. al., 2006; Verbiest et.al., 2009), ATR remains one of the most reliable techniques. Thin film samples of C1 were electric field poled at various applied voltages to obtain a linear relationship between r_{33} and applied poling field strength (E_p , in units of V/micron). C1 was demonstrated to give r_{33} values ~ 140 pm/V, three times higher than that of the same chromophore core (FTC-type) in an amorphous polymer host at optimal (20% chromophore) number density (Benight et. al., 2010). C1 is 41% chromophore and spin coated neat with no host. In addition, the poling efficiency for C1 on TiO₂-coated substrates was measured to be $r_{33}/E_p = 1.92$ (Benight et. al., 2010).

2.3 Molecular order of C1

Upon observing that C1 exhibited superior EO activity (greater than what would be expected with simply increasing the number density), methods which could ascertain the degree of poling-induced order, $\langle P_2 \rangle$, were employed. $\langle P_2 \rangle$ is related to $\langle \cos^2 \theta \rangle$, the second degree order parameter through Eq. 6

$$\langle P_2 \rangle = \frac{3 \langle \cos^2 \theta \rangle - 1}{2} \quad (6)$$

Currently, no direct method for measuring acentric order, $\langle \cos^3 \theta \rangle$, in a material system is available. To obtain a quantitative measurement of acentric order in the system, other components of the r_{33} equation must be calculated and $\langle \cos^3 \theta \rangle$ back-calculated from knowledge of the other parameters. However, the $\langle P_2 \rangle$ or the centric (order) of molecules can be measured using several experimental methods. The normal incidence method (NIM), in which UV-visible absorption spectra are acquired at normal to the surface of the chromophore sample before and after poling, has been employed (Kim et. al, 2009; Benight et. al., 2010). The $\langle P_2 \rangle$ is able to be measured based on the assumption that as strongly absorbing chromophore molecules are poled in the z direction of the substrate, the chromophores orient more parallel to the poling axis, therefore absorbing less in the plane of the substrate. While the NIM does yield insight into the centrosymmetric order of materials, the measurement is simple and prone to error in that photo-induced chromophore degradation can lead to significant over-estimation of poling-induced order.

Recently, new and improved methods for measuring $\langle P_2 \rangle$ of EO materials have been introduced. The method developed by Robinson and coworkers is known as Variable Angle Polarization Referenced Absorption Spectroscopy (VAPRAS) and measures, at various angles of incidence, absorption of s and p polarizations of light (Olbricht et. al., 2011). Utilization of the ratio of s and p absorptions negates and attenuates the effects of Fresnel reflections. That is, the s polarized absorption acts as a reference. The C1 material was studied using NIM and VAPRAS techniques to yield $\langle P_2 \rangle$ values of $\langle P_2 \rangle = 0.16$ and $\langle P_2 \rangle = 0.19$, respectively for samples poled at 50 V/micron (Benight et. al., 2010).

While the absorption of the chromophore unit of the C1 molecule could be easily probed due to being in a desirable wavelength range for the VAPRAS instrument, the absorption profiles of the coumarin units after poling remained inaccessible. Utilizing another technique capable

of ascertaining absorption behavior over a wide range of wavelengths (190nm -1700nm), Variable Angle Spectroscopic Ellipsometry (VASE) was employed for unpoled and poled samples of C1 (Woollam, 2000). Isotropic and anisotropic models can both be applied to analyze optical constants of samples. In our case, an anticipated anisotropy in the xz , yz (poling) axes prompted us to use an anisotropic model for samples that have been poled. Using an anisotropic model, the absorptions of the coumarin and chromophore units were able to be obtained for both the plane perpendicular to the sample surface (as studied in UV-Vis absorption spectroscopy) and for the plane within the sample (Benight et. al., 2011). A clear illustration of the absorption profiles as measured with VASE is given in Fig. 5.

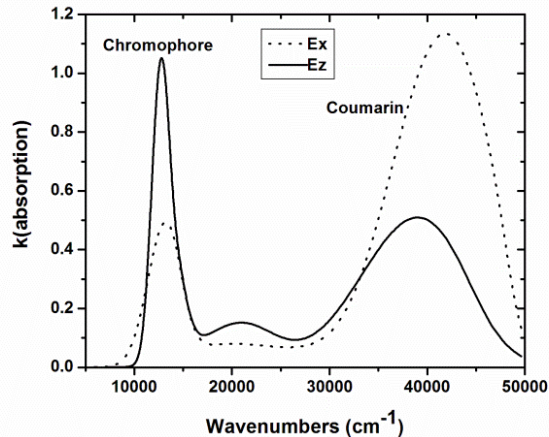


Fig. 5. The absorption component of the refractive index, k , is shown for representative samples of the C1 system. Absorption in the x -plane is shown by the dotted line while absorption containing the z -plane is shown by the solid line

These results illustrate that the coumarin units in poled samples of C1 were oriented in the x - y planes of the sample, orthogonal to that of the chromophores.

Not only can VASE be used to detect absorption behavior for a wide range of transparent and absorptive materials, but VASE can also be used to compute the $\langle P_2 \rangle$ of a material using Eq. 7.

$$\langle P_2 \rangle = \frac{k_p - k_{\perp}}{k_p + 2k_{\perp}} \quad (7)$$

Here, the k_p coefficient represents the absorption parallel to the normal of the film (z axis) and k_{\perp} represents the absorption perpendicular to the poling (z) axis (Michl & Thulstrup, 1986). The $\langle P_2 \rangle$ for samples of C1 poled at 50 V/micron was measured to be $\langle P_2 \rangle = 0.24$, in good agreement with VAPRAS measurements of the material (Benight et. al., 2011; Benight, 2011). In addition, the $\langle P_2 \rangle$ of the coumarin units was found to be $\langle P_2 \rangle = -0.19$. Since mathematically, the highest negative order that can be achieved is $\langle P_2 \rangle = -0.5$, the coumarins are approximately $\sim 40\%$ centrosymmetrically ordered in the xy plane (Benight et. al., 2011; Benight, 2011).

2.4 BCOG system incorporating C1

A BCOG system including the C1 material as a chromophore-containing host and a guest chromophore (polyene bridge, CLD-based) was also characterized. The guest chromophore YLD-124 (CLD-type) was doped at 25 wt % into C1 and spin coated onto TiO₂ coated ITO glass substrates. From poling experiments and measurements of EO activity using ATR technique, the poling efficiency (r_{33}/E_p) was measured to be 2.00, slightly higher than the poling efficiency for neat C1 at $r_{33}/E_p = 1.92$ (Benight et. al., 2010). This poling efficiency is a bit lower compared to other BCOG systems, but a small enhancement is still observed (Kim et. al., 2008). The lack of more improved enhancement in the BCOG system with C1 as a host is likely due to the addition of more chromophore molecules complicating the reduced fractional lattice dimensionality experienced by the chromophores in C1. The addition of more chromophores is likely restricting coumarin movement slightly, but the restriction in chromophore movement from fractional lattice dimensionality imposed on the chromophores is likely already fully reached with the neat C1 system.

2.5 Investigation of molecular cooperativity and mobility in C1

Intermolecular electrostatic interactions leading to improved poling-induced order should also be manifested through impact on viscoelastic properties. Traditionally, differential scanning calorimetry (DSC) is a method for ascertaining thermal transitions in a material. Upon DSC investigation of C1, it was observed that a glass transition-like change was apparent around 80 °C.

To probe the thermal transitions on a more sensitive scale, we employed methods capable of detecting molecular mobility and cooperativity on the nanoscale. Length scales and degrees of cooperativity (quantitative energetics of activations of various phases) can be deduced by nanoviscoelastic and nano-thermorheological measurements. The nanoscopic methods of Shear Modulation Force Microscopy (SM-FM), Intrinsic Friction Analysis (IFA) and Dielectric Relaxation Spectroscopy (DRS) were used to examine C1. These methods have also been applied to EO systems which incorporate Ar-pFAR pendant group interactions (Gray et. al., 2007, 2008; Zhou et. al., 2009; Knorr et. al., 2009b).

Before proceeding with the results of the C1 system, it is important to give a brief overview of each of these instruments. SM-FM is a nanoscopic analogue to dynamic mechanical analysis (DMA) widely used in studies of the nanoviscoelastic behavior of polymer relaxations and phase behavior. The SM-FM instrument is essentially an Atomic Force Microscope that measures the temperature-dependent shear force on a tip modulated parallel to the sample surface (Ge et. al., 2000). SM-FM measures the force required to move the tip of contact and the velocity of the moving tip at fixed temperatures. Experiments are typically acquired at increments of 1 K temperature. These perturbations in force and velocity can be quantified in a contact stiffness parameter (typically denoted as k_c). As the experiment is carried out over a range of temperatures, changes in the slope of contact stiffness versus temperature yield information about temperatures at which phase transitions in the material occur.

In order to ascertain specific information regarding the energetics of the detectable phase transitions as found in the SM-FM measurements, IFA was employed. IFA is a nanoscopic analogue based on the well-known lateral force microscopy technique capable of providing

molecular descriptions of relaxation processes associated with transitions of structural molecular movement (Knorr et. al., 2009a). From the IFA experiment, quantitative energies of activation for structural transitions, referred to as “apparent energy” or E_a , and the molecular-scale cooperativity of these transitions can be measured. Non-cooperative processes are generally described taking into account dynamic enthalpy ΔH solely. However, if a process is cooperative, the dynamic entropy (ΔS) is also taken into account as given in the classical sense from Gibbs Free energy, $\Delta G^* = \Delta H^* - T\Delta S^*$. In addition to IFA measuring E_a , the technique also measures $T\Delta S^*$.

The IFA technique utilizes the same instrument as in SM-FM. Specifically, the force required to move the tip probe from the AFM is measured at a fixed temperature to give a force curve as a function of the log of the velocity. Data are shifted to achieve a “master” curve according to the time-temperature equivalence principle (Ward, 1971; Ferry, 1980). The vertical shifting of data is related to $T\Delta S^*$ in the Gibbs energy and depicts the degree of cooperativity as observed with respect to temperature for the material. It can be valuable to also estimate the contribution due to entropic energy from the measurement. To conduct this exercise, a method developed by Starkweather can be used to analyze the cooperativity with apparent Arrhenius activation energies which can be determined from Eq. 8 (Starkweather, 1981, 1988).

$$E_a = RT \cdot \left[1 + \ln \left(\frac{kT}{2\pi h f_0} \right) \right] + T\Delta S^* \quad (8)$$

where k and h are Boltzmann’s constant and Plank’s constant, respectively, and f_0 is the frequency at which the relaxation peak is observed. f_0 is either deduced from DRS or estimated (Sills et. al., 2005). In IFA, the friction force typically varies with temperature and the velocity at which the tip moves is accounted for using the WLF superposition (Williams et. al., 1955).

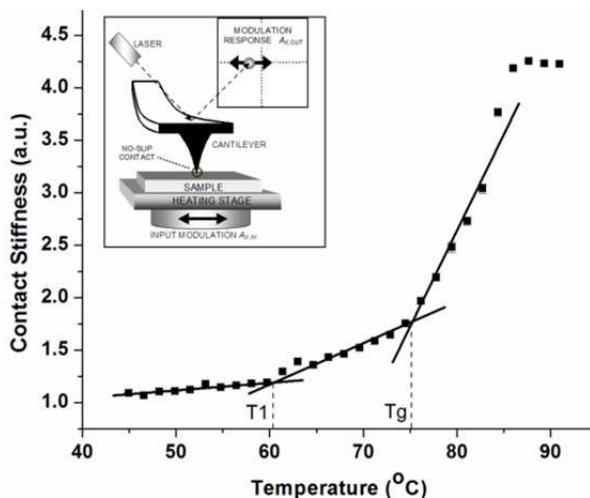


Fig. 6. SM-FM example data of the C1 system. T_1 and T_g are labeled for clarity. A schematic of the SM-FM instrument is given in the inset

In conducting SM-FM and IFA measurements for C1, two distinct thermal transitions were observed for the samples of C1. The first transition, denoted as T_1 , was observed at 61 °C and a transition quite close to the T_g (at 76 °C), denoted as T_2 , was also observed. An example SM-FM scan for C1 is given in Fig. 6.

The T_1 transition was not detectable clearly in the DSC scan, however was able to be probed nanoscopically using SM-FM. The results from the SM-FM and IFA for the C1 system and the molecule HD-FD (incorporating Ar-pFA interactions) is presented for comparison.

	Temperature Range	E_a [kcal/mol] ^a	$T\Delta S^*$ [kcal/mol] ^b
C1	$T < T_c$	16±3	-
	$T_c < T < T_g$	43±4	-
	$T > T_g$	72±4	54-58
HDFD	$T < T_c$	23	-
	$T_c < T < T_g$	44	-
	$T > T_g$	71	52-56

Table 1. The activation energies of HDFD and C1. ^a IFA results. ^b Estimated from Eq. 8.

Above the glass transition temperature, the mobility of the chromophore molecules in the system is the highest allowing for maximum cooperativity in the system. In fact, the entropic component of the activation energy is 75-80% of the activation energy above T_g . The vertical friction shift, related to molecular cooperativity is shown for the C1 compound in Fig. 7 below.

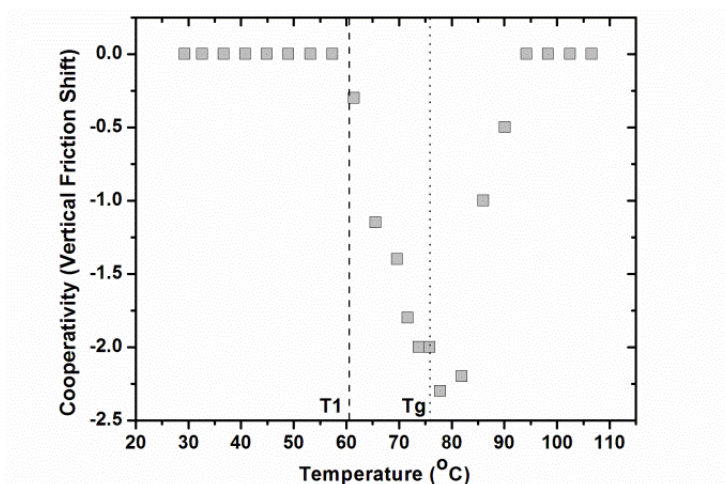


Fig. 7. The vertical friction shift, related to molecular cooperativity, is shown for C1. The plot shows that cooperativity starts at the T_1 temperature and is maximized at the glass transition or poling temperature of the material

Keeping in mind that this plot is proportional to the change in entropy and signifies the molecular cooperativity in the material, the cooperativity in C1 starts to increase at T_1 and

reaching a maximum at T_g . IFA data yield an associated activation entropy change, $|\Delta S| \sim 160$ cal/K for C1 (Benight et. al., 2011; Benight, 2011).

Another method that works in tandem with IFA in providing critical information on the length scales of molecular cooperativity is that of dielectric relaxation spectroscopy (DRS). Specifically the dissipation length, $\xi(T)$ for cooperativity or molecular mobilities (molecular interactions) can be quantified. The dissipation length is determined from Eq. 9.

$$\xi(T) = v_p(T)/f_p(T) \quad (9)$$

where $v_p(T)$ is the peak velocity from IFA and $f_p(T)$ is the peak relaxation frequency determined from DRS (Sills et. al., 2005, Hedvig, 1977). In the actual measurement, the real and imaginary impedance values are measured and are given in Eqs. 10 and 11. These values are ascertained for a range of frequencies and temperatures. By measuring the real and imaginary values of the impedance, information of the real and imaginary portions of the dielectric data are known.

$$\varepsilon'(\omega) = \frac{-Z''}{\omega C_0(Z'^2 + Z''^2)} ; \varepsilon''(\omega) = \frac{Z'}{\omega C_0(Z'^2 + Z''^2)} \quad (10,11)$$

where C_0 is the vacuum capacitance of the test set-up without the sample, and ω is the angular frequency. It's important to note that in the measurement referred to here, poled samples of OEO materials are measured (in a parallel plate capacitor format).

Eq. 9 is used to acquire a dissipation length for the material, however, it can be difficult to obtain $v_p(T)$ and $f_p(T)$ at the same temperatures over large ranges of temperature. This limits the amount of information to be acquired at lower temperatures closer to T_g , however, information from both IFA and DRS can be acquired at temperatures above T_g and cooperativity can be extrapolated to lower temperatures.

It is important to note that the DRS technique is widely applied in the study of polymer relaxations, side-chain and main-chain relaxations in particular, but this technique has rarely been shown to be used on organic molecular glassy systems like C1. The dissipation length for C1 was measured to be as high as 55 ± 25 nm at 106°C , approximately 25°C above the T_g of the material as measured by DSC and SM-FM (Benight, 2011). To compare to other materials, typically the dissipation length for polystyrene, a conventional polymer, fades to a couple of angstroms at temperatures above T_g . As another comparison, an EO material containing Ar-pFAR interactions was analyzed using the same DRS instrument used in the investigation of C1 to give $\xi = 15 \pm 10$ nm at $T = 153 - 160^\circ\text{C}$ (Knorr, 2010). The higher dissipation length for C1 likely indicates that the interactions in C1 are more stable over longer length scales. Furthermore, this dissipation length signifies that in the C1 system, the movement of one C1 molecule is influenced by another C1 molecule up to approximately 55 nm away.

2.6 Reduced dimensionality

The C1 material system has been shown to exhibit increased centrosymmetric and acentric order, intermolecular coumarin pendant group interactions and defined optical orthogonal orientations of chromophore and coumarin units (Benight et. al., 2010). These results can be

explained as the coumarin-based pendant groups imposing a lattice restriction which leads to fractional dimensional order of the chromophore molecules in the presence of an electric poling field. Inflicting a dimensional restriction upon the chromophores increases centrosymmetric order and may also increase acentric order of the bulk material system, at constant poling field strength. This lattice dimensionality restriction, as applicable to the chromophore systems presented here, can be described utilizing two different theoretical arguments both using the independent particle assumption in a low-density limit (Benight et. al., 2010). The fundamental statistical description of the order parameters is defined in Eq. 12.

$$\langle \cos^n \theta \rangle = \frac{\iint_{\theta, \phi} \cos^n \theta P(\theta, \phi) e^{\frac{\mu \cdot E_0}{kT}} d\cos\theta d\phi}{\iint_{\theta, \phi} P(\theta, \phi) e^{\frac{\mu \cdot E_0}{kT}} d\cos\theta d\phi} \quad (12)$$

where the probability distribution is given in Eq. 13 and is described using the many-body interactions potential (the Hamiltonian) (Benight et. al., 2010).

$$P(\theta, \phi) = \frac{e^{-\frac{H^0}{kT}}}{\iint_{\theta, \phi} e^{-\frac{H^0}{kT}} d\cos\theta d\phi} \quad (13)$$

The $f = \frac{\mu E_0}{kT}$ term indicates the statistical weight representing the dipole interaction with the homogenous poling field, E_0 . It is important to note that the E_0 given in Eq. 12 is representative of the electric field at the chromophore molecule and does not necessarily represent the overall applied poling field strength (E_p).

In the first theoretical treatment the ordering potential is considered to be uniform but the dimensionality, M , of the space is reduced. In this case the order parameter is computed using Eq. 14 (Stillinger, 1977).

$$\langle \cos^n \theta \rangle_M = \frac{\int_{\theta} \cos^n \theta e^f \sin^{M-2} \theta d\theta}{\int_{\theta} e^f \sin^{M-2} \theta d\theta} \quad (14)$$

This expression is easily solved in terms of Bessel functions, $I_\nu(f)$. For example, the lowest indexed order parameter, $n=1$, is computed from Eq. 15.

$$\langle \cos \theta \rangle_M = \frac{I_M(f)}{I_{M-1}(f)} \quad (15)$$

All higher index order parameters can be found from this one and its derivatives. In this theoretical treatment, different dimensional restrictions translate to varied degrees of rotation for the point dipoles in the system. In this model, in three dimensions, the dipolar molecule being examined can access any orientation in the Cartesian coordinate system exhibiting Langevin type behavior. By generalizing the Langevin function for any dimension, we can describe molecular order for any fractional dimension from 1 to 3 dimensions. Full derivation for the equations for 2D and 3D scenarios and 2nd degree (centrosymmetric) and 3rd degree (acentric) order parameters has been given previously (Benight et. al., 2010).

The centrosymmetric and acentric order parameters give insight into the system's dimensionality. The dimensional restrictions given for a single dipole can translate to dimensionality of molecules (chromophores in our case) in macroscopic systems including those restrictions originating from the environment. The dimensionality, M , can be approximated from a linear interpolation between $M = 2$ and $M = 3$ from the relation of $\langle \cos^3 \theta \rangle / \langle P_2 \rangle$, as shown in Eq. 16 (Benight et. al., 2010).

$$\langle \cos^3 \theta \rangle_{MD} \approx \sqrt{\left(\frac{9-2M}{2+M} \right) \left(\langle P_2 \rangle_{MD} - \frac{3-M}{2M} \right)} \quad (16)$$

Using this linear interpolation model, the dimensionality of C1 was found to be $M = 2.2$ D while those of the control systems utilizing more standard conventional chromophore systems with the same chromophore core were nearly 3D (Benight et. al., 2010). Such results have been corroborated by theoretical modeling of chromophores including rigid body Monte Carlo (RBMC) methods, in which the dimensional restriction was observed at experimental densities similar to that of C1 (see next section).

For the second model, called the Rigid Wall Model, a similar theoretical description of dimensionality emerges. In the rigid wall model, the order parameters of the dipoles can be defined from a simple distribution generated by a confining potential in which the dipoles may rotate unimpeded up to a stop angle, $q_0 = \cos \theta_{stop}$. The stopping angle is related to the dimensionality by Eq. 17.

$$q_0(1 + q_0) = \left(\frac{3 - M}{M} \right) \quad (17)$$

When this description of the confining potential is substituted into Eq. 12, the acentric order parameter for the lowest order, $n=1$, is given according to Eq. 18.

$$\langle \cos \theta \rangle = \frac{\cosh(f) - q_0 \cosh(q_0 f)}{\sinh(f) - \sinh(q_0 f)} - \frac{1}{f} \quad (18)$$

Again, all other order parameters can be found from this one and appropriate derivatives. An illustration of the ratio of centric ($\langle P_2 \rangle$) to acentric ($\langle \cos^3 \theta \rangle$) order parameters for all of the theoretical descriptions of dimensionality that have been presented here can be of utility. Fig. 8 illustrates the relationship of $\langle P_2 \rangle$ and $\langle \cos^3 \theta \rangle$ for several different dimensionalities. Overlaid in Fig. 8 are (1) the linear interpolation of the two order parameters as derived

from Bessel functions (red dotted line), (2) the dimensionality as computed from Bessel $I(z)$ functions (black solid line) and (3) the dimensionality as computed from the rigid wall model of confining potential (blue solid line).

Fig. 8 shows that for as the dimensionality is less restricted (ascending toward $N = 3$), the relationship between $\langle P_2 \rangle$ and $\langle \cos^3 \theta \rangle$ is the same for all of the theoretical models. All three models agree nicely for dimensionalities from $N = 3$ to $N = 2$, however, as the dimensionality is further restricted toward 1.1 D, the theoretical model which utilizes a linear interpolation of $\langle P_2 \rangle$ and $\langle \cos^3 \theta \rangle$ to calculate dimensionality is not as aligned with the other two models.

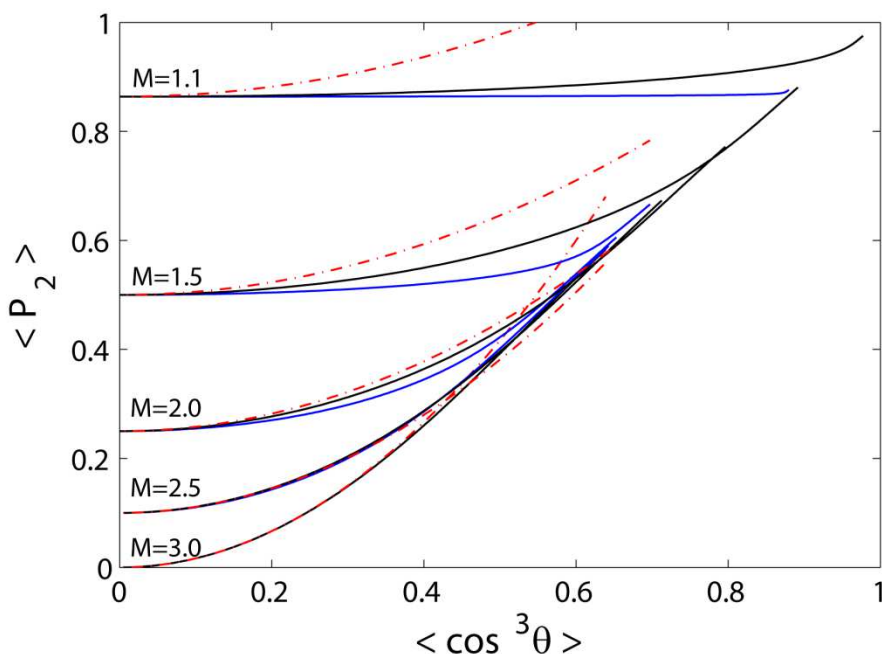


Fig. 8. The relationship of $\langle P_2 \rangle$ to $\langle \cos^3 \theta \rangle$ is presented for different dimensionalities. The methods for computing lattice dimensionality presented above are overlaid in the plot for specific quantitative dimensional systems (e.g. $N = 3.0$, $N = 2.5$, $N = 2.0$, $N = 1.5$, $N = 1.1$). The red dotted line illustrates the dimensionality as computed using the linear interpolation from Eq. 16. The black solid line illustrates the dimensionality as computed from Bessel $I(z)$ functions and the blue solid line represents the rigid wall model (the second method presented above)

In summary, the reduced dimensionality integrals are easily represented by Bessel functions, making the computation of the order straightforward, and are easily compared to a full 3D model with a restrictive wall barrier characterized by a designated cutoff angle. These models of dimensionality show that achieving reduced lattice dimensionality for a material system encompassing strongly dipolar chromophores will increase centrosymmetric order and may also increase acentric order at the same poling strength

being applied to the system. Furthermore, one can compare $\langle P_2 \rangle$ and $\langle \cos^3 \theta \rangle$ to determine whether the effective dimensionality of the material system has been reduced.

2.7 Theoretical methods

Theoretical methods coupled with experimental results have been integral in understanding molecular interactions in systems such as C1. The specific theoretical methods of rigid body Monte Carlo (RBMC), fully atomistic Monte Carlo (FAMC) and molecular dynamics (MD) have been crucial (Sullivan et. al., 2009; Rommel & Robinson, 2007; Robinson & Dalton, 2000; Benight et. al, 2010; Leahy-Hoppa et. al., 2006; Knorr et. al., 2009b). Such methods have been used to study EO dendrimer, chromophore guest polymer host systems, BCOGs and MAP systems. With custom code, an electric field poling experiment can be simulated with an ensemble of ellipsoids or spheres parameterized to possess the properties of the experimental chromophore systems and 1st, 2nd, and 3rd degree order parameters can be computed. Such capability allows the effect of different applied poling field strengths, different temperatures on chromophores systems and various sizes and shapes of ellipsoids to be investigated (Benight et. al., 2010).

RBMC simulations were implemented in investigation of the effect of density of chromophores systems on centrosymmetric (2nd degree) and acentric (3rd degree) order. As part of this investigation, prolate ellipsoids parameterized as the F2 chromophore (the active chromophore unit in C1, depicted in Fig. 1) were simulated under applied poling fields of 50 V/micron and 75 V/micron at low densities of chromophores in the system (~20%) ranging upwards of 60% chromophore (Benight et. al., 2010). The $\langle P_2 \rangle$ and $\langle \cos^3 \theta \rangle$ values were computed for each simulation and the dimensionalities of the simulations from these order computations were determined. The results of these simulations illustrated that at low numbers density (~20%) in electrically-poled guest-host systems, nearly no dimensional restriction exists, yielding nearly three dimensional systems. However, upon increasing the number density of the system toward number densities of chromophore concentration similar to that of C1 (40% and beyond) the centric order of the chromophores as observed from the computed $\langle P_2 \rangle$ values and visualizations of the simulations increased dramatically (Benight et. al., 2010). At nearly 60% chromophore concentration, the visualization of the simulation showed a system that closely resembles that of a smectic-A liquid crystal with high planar and directional order (Benight et. al., 2010). Furthermore, the dimensionality of this system was calculated to be less than 2, indicating more dimensional restriction at

E_p (V/ μ m)	N^a	$\langle P_2 \rangle$	$\langle \cos^3 \theta \rangle$	M
50	1.26	0.015 ± 0.001	0.052 ± 0.0001	2.9
	2.52	0.017 ± 0.003	0.046 ± 0.0003	2.9
	3.78	0.017 ± 0.003	0.040 ± 0.0002	2.9
	5.04 ^b	0.042 ± 0.007	0.035 ± 0.0003	2.8
	6.30 ^b	0.42 ± 0.11	0.013 ± 0.001	< 2

Table 2. RBMC simulation results for ellipsoids under an electric poling field of $E_p = 50$ V/micron parameterized as the chromophore cores in C1. $T = 382$ K, $m = 1728$ particles. ^a($\times 10^{20}$ molecules/cc); ^bLonger runs were required for convergence at these densities

increasing number densities of chromophore concentration. (Note: in RBMC simulations, the coumarin pendant groups in MAP systems are not taken into account). Results from the simulations are given in Table 2 for clarity.

In the most recent development of molecular dynamics of chromophore systems, the C1 chromophores are parameterized with the MMFF94 force field (Halgren, 1996) and MD simulations were run using the Tinker 5.1 program (Ponder, 2010) and simulated in a defined box with an Ewald boundary. Simulations can be run at room temperature or at appropriate poling temperatures near T_g (Benight et. al., 2011; Benight, 2011).

A standard statistical mechanical correlation function (McQuarrie, 2000) can be used to monitor the interactions of chromophore components in the simulation. The correlation function used in an example of recent work is given in Eq. 19 (Benight et. al., 2011; Benight, 2011).

$$g(r) = \frac{V \sum_i^N \sum_{j>i}^N n_{ij}(r, r + dr)}{2\pi N(N-1)r^2 dr} \quad (19)$$

In this equation, the volume of the system (V), the number of molecules in the system (N) and the distance between two components, r are accounted for and are indicative of the radial distribution. In the simulation of molecules specific intermolecular interactions can be probed by monitoring a given atom in the molecule of interest. For example, in the C1 system, the sulfur atom on the thiophene component of the bridge can be tagged and the interactions between intermolecular S-S can be quantified, enabling probing of the chromophore-chromophore interactions in the system. Furthermore, monitoring a specific carbonyl group of the coumarin pendant group enables monitoring of intermolecular interactions between neighboring pendant groups. The correlation function allows for monitoring at varied distances apart (Benight et. al., 2011; Benight, 2011).

As an example, MD, simulations of C1 can be run in the presence of chloroform molecules and as neat systems at experimental density. Upon viewing simulation visualizations of these simulations, the correlation functions demonstrate that in the C1 system, the chromophore-chromophore dipole-dipole interactions as monitored through the S-S bonds in the chromophore units are suppressed when compared to runs of just the chromophores in the simulation and in runs including short PMMA polymer chains in the simulation. Furthermore, distinct coumarin-coumarin interactions are evident and constant for various concentrations. In addition, visualizations of the simulations illustrate coumarin-coumarin pairs or dimers that regularly occur, further driving home the point that the intermolecular interactions of the coumarin have a strong presence in the C1 system. An example visualization of simulated neat C1 using MD is shown in Fig. 9.

In addition to MD, fully atomistic Monte Carlo (FAMC) can be employed in the study of OEO chromophore systems. It has been demonstrated that simulation under a poling field of EO chromophore dendrimers are quite useful in investigating the order parameters and poling behavior. Recent code development upgrades (done in-house) also enable the study of systems like C1 in which several levels of detail are possible in simulation the chromophores. Ellipsoids can be parameterized around the chromophore and coumarin

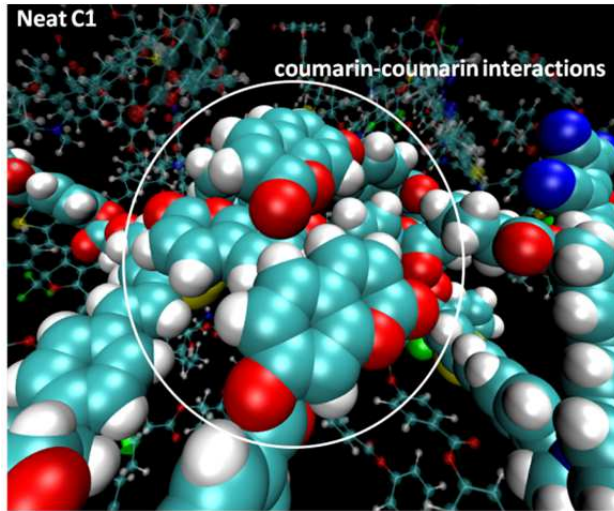


Fig. 9. A visualization of the C1 molecule as observed in the MD simulations shown

units, around specific functional units or groups within those components, or around every aromatic ring to yield further levels of detail in modeling of the chromophores. Indeed, with more levels of detail, more simulation time and expense arise. Results with updated code are still primitive, but this approach bodes well for being able to simulate more complex systems in the future.

3. Conclusions

A combination of methods for characterization of soft matter organic electro-optic materials can be utilized to yield insight into molecular order, material performance, and intermolecular interaction dynamics. The specific methods of attenuated total reflection (ATR) and *in-situ* poling are of utility for measuring the EO activity of OEO materials. Techniques such as shear-modulation force microscopy (SM-FM), intrinsic friction analysis (IFA) and dielectric relaxation spectroscopy (DRS) determine viscoelastic properties of the materials. These methods yield insight into the dynamics of intermolecular interactions in the material system, including measurement of the quantitative energies of activation for the materials discussed. In addition, optical spectroscopy methods such as Variable Angle Spectroscopic Ellipsometry (VASE) were utilized to probe the unique molecular orientations of chromophore and coumarin units in the C1 system. These experimental methods can be coupled with theoretical methods such as Monte Carlo and Molecular Dynamics to further understand the molecular ordering and intermolecular interactions in the C1 system. Utilizing all of these methods together illustrates that the coumarin-based pendant groups of the C1 molecule interact in a plane orthogonal to the chromophores to enhance the acentric order of the EO active chromophores in the presence of a poling field. It has been shown that this result can be explained through reduced dimensionality in that the coumarins are imposing a dimensional restriction on the lattice environment in which the chromophores are embedded, yielding higher centric and acentric order in the system. These results of higher order, in turn, lead to enhanced EO activities.

Utilizing this approach of nano-engineering intermolecular interactions for enhanced molecular order will aid in the development of improved OEO materials. Understanding the role and effect of intermolecular interactions yields higher EO activities. If EO performance continues to be improved, OEO materials can potentially replace the current inorganic materials being utilized in commercial applications. Such materials, for example, can be implemented into hybrid silicon-organic nano-slot waveguide device structures which, if incorporated successfully with OEO materials, could revolutionize the telecommunications industry with the ultrafast transmission of information.

4. Acknowledgments

Lewis Johnson, Prof. Antao Chen, Prof. Bruce Eichinger, Dr. Philip Sullivan, Dr. Dan Knorr, Prof. Rene Overney, Dr. Sei-hum Jang, Dr. Jingdong Luo, Su Huang and Andreas Tillack are thanked for useful discussions and assistance with experiments and calculations. Funding from the NSF [DMR-0120967] and the AFOSR [FA9550-09-0682] are gratefully acknowledged.

5. References

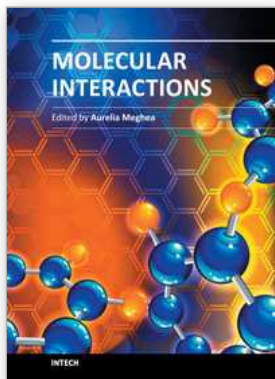
- Baehr-Jones, T.; Penkov, B.; Huang, J.; Sullivan, P. A.; Davies, J.; Takayesu, J.; Luo, J.; Kim, T. D.; Dalton, L. R.; Jen, A. K.-Y.; Hochberg, M.; Scherer, A. (2008) Nonlinear polymer-clad silicon slot waveguide modulator with a half wave voltage of 0.25 V. *Applied Physics Letters*, Vol.92, No.7, pp. 163303-1-3.
- Benight, S. J.; Bale, D. H.; Olbricht, B. C.; Dalton, L. R. (2009) Organic electro-optics: Understanding material structure/function relationships and device fabrication issues. *J. Mater. Chem.*, Vol.19, pp. 7466-7475.
- Benight, S. J.; Johnson, L. E.; Barnes, R.; Olbricht, B. C.; Bale, D. H.; Reid, P. J.; Eichinger, B. E.; Dalton, L. R.; Sullivan, P. A.; Robinson, B. H. (2010) Reduced Dimensionality in Organic Electro-Optic Materials: Theory and Defined Order. *J. Phys Chem. B.*, Vol.114, No.37, pp. 11949-11956.
- Benight, S. J.; Knorr, D. B., Jr.; Sullivan, P. A.; Sun, J.; Kocherlakota, L. S.; Robinson, B. H.; Overney, R. M.; Dalton, L. R. (2011) Nano-Engineering of Soft Matter Lattice Dimensionality: Measurement of Nanoscopic Order and Viscoelasticity, *Submitted*.
- Benight, S. J. (2011) Nanoengineering of Soft Matter Interactions in Organic Electro-Optic Materials. University of Washington, Seattle, WA, USA.
- Blanchard-Desce, M.; Baudin, J.-B.; Jullien, L.; Lorne, R.; Ruel, O.; Brasselet, S.; Zyss, J. (1999) Toward highly efficient nonlinear optical chromophores: molecular engineering of octupolar molecules. *Opt. Mater.*, Vol.12, pp. 333-338.
- Chen, A.; Chuyanov, V.; Garner, S.; Steier, W. H.; Dalton, L. R. (1997) Modified attenuated total reflection for the fast and routine electro-optic measurement of nonlinear optical polymer thin films. *Organic Thin Films for Photonics Applications, 1997 OSA Technical Digest Series*, Vol.14, pp. 158-160.
- Cheng, Y.-J.; Luo, J.; Hau, S.; Bale, D. H.; Kim, T.-D.; Shi, Z.; Lao, D. B.; Tucker, N. M.; Tian, Y.; Dalton, L. R.; Reid, P. J.; Jen, A. K.-Y. (2007) Large Electro-optic Activity and Enhanced Thermal Stability from Diarylamino-phenyl-Containing High- β Nonlinear Optical Chromophores. *Chem. Mater.* Vol.19, pp. 1154-1163.

- Cheng, Y.-J.; Luo, J.; Huang, S.; Zhou, X.; Shi, Z.; Kim, T.-D.; Bale, D. H.; Takahashi, S.; Yick, A.; Polishak, B. M.; Jang, S.-H.; Dalton, L. R.; Reid, P. J.; Steier, W. H.; Jen, A. K. Y. (2008) Donor-Acceptor Thiolated Polyenic Chromophores Exhibiting Large Optical Nonlinearity and Excellent Photostability. *Chem. Mater.*, Vol.20, No.15, pp. 5047-5054.
- Dalton, L. R.; Sullivan, P. A.; Bale, D. H. (2010) Electric Field Poled Organic Electro-Optic Materials: State of the Art and Future Prospects *Chem. Rev.*, Vol.110, pp. 25-55.
- Dalton, L. R.; Benight, S. J.; Johnson, L. E.; Knorr, D. B., Jr.; Kosilkin, I.; Eichinger, B. E.; Robinson, B. H.; Jen, A. K.-Y.; Overney, R. M. (2011) Systematic Nanoengineering of Soft Matter Organic Electro-optic Materials. *Chem. Mater.*, Vol.23, 3, pp. 430-445.
- Dalton, L. R.; Benight, S. J. (2011) Theory-Guided Design of Organic Electro-Optic Materials & Devices. *Polymer*, Vol.3, No.3, pp. 1325.
- Davies, J. A.; Elangovan, A.; Sullivan, P. A.; Olbricht, B. C.; Bale, D. H.; Ewy, T. R.; Isborn, C. M.; Eichinger, B. E.; Robinson, B. H.; Reid, P. J.; Li, X.; Dalton, L. R. (2008) Rational Enhancement of Second-Order Nonlinearity: Bis-(4-methoxyphenyl)hetero-aryl-amino Donor-Based Chromophores: Design, Synthesis, and Electrooptic Activity. *J. Am. Chem. Soc.*, Vol.130, No.32, pp. 10565-10575.
- Ding, R.; Baehr-Jones, T.; Liu, Y.; Bojko, R.; Witzens, J.; Huang, S.; Luo, J.; Benight, S.; Sullivan, P.; Fedeli, J.-M.; Fournier, M.; Dalton, L.; Jen, A.; Hochberg, M. (2010) Demonstration of a low V_{πL} modulator with GHz bandwidth based on electro-optic polymer-clad silicon slot waveguides. *Opt. Express*, Vol.18, No.15, pp. 15618-15623.
- Enami, Y.; Mathine, D.; Derose, C. T.; Norwood, R. A.; Luo, J.; Jen, A. K.-Y.; Peyghambarian, N. (2007) Hybrid cross-linkable polymer/sol-gel waveguide modulators with 0.65 V half wave voltage at 1550 nm. *Appl. Phys. Lett.*, Vol.91, pp. 093505.
- Facchetti, A.; Annoni, E.; Beverina, L.; Morone, M.; Zhu, P.; Marks, T. J.; Pagani, G. A. (2004) Very large electro-optic responses in H-bonded heteroaromatic films grown by physical vapour deposition. *Nature Mater.*, Vol.3, pp. 910-917.
- Ferry, J. D. (1980) Ch11: Dependence of viscoelastic behavior on temperature and pressure. In *Viscoelastic Properties of Polymers*, John Wiley & Sons; pp 265-320.
- Frattarelli, D.; Schiavo, M.; Facchetti, A.; Ratner, M. A.; Marks, T. J. (2009) Self-Assembly from the Gas-Phase: Design and Implementation of Small-Molecule Chromophore Precursors with Large Nonlinear Optical Responses. *J. Am. Chem. Soc.* Vol.131, No.35, pp. 12595-12612.
- Ge, S.; Pu, Y.; Zhang, W.; Rafailovich, M.; Sokolov, J.; Buenviaje, C.; Buckmaster, R.; Overney, R. M. (2000) Shear modulation force microscopy study of near surface glass transition temperature. *Phys. Rev. Lett.*, Vol.85, No.11, pp. 2340-2343.
- Gray, T.; Killgore, J. P.; Luo, J.; Jen, A. K.-Y.; Overney, R. M. (2007) Molecular mobility and transitions in complex organic systems studied by shear force microscopy. *Nanotechnology*, Vol.18, pp. 044009.
- Halgren, T. A. (1996) Merck Molecular Force Field. I. Basis, Form, Scope, Parameterization, and Performance of MMFF94*. *J. Comput. Chem.*, Vol.17, No.5-6, pp. 490.
- Hammond, S. R.; Clot, O.; Firestone, K. A.; Bale, D. H.; Lao, D.; Haller, M.; Phelan, G. D.; Carlson, B.; Jen, A. K. Y.; Reid, P. J.; Dalton, L. R. (2008) Site-Isolated Electro-optic Chromophores Based on Substituted 2,2'-Bis(3,4-propylenedioxythiophene) π -Conjugated Bridges. *Chem. Mater.* Vol.20, No.10, pp. 3425-3434.

- Hedvig, P. (1977) *Dielectric spectroscopy of polymers*. 1st ed.; John Wiley & Sons: New York.
- Herminghaus, S.; Smith, B. A.; Swalen, J. D. (1991) Electro-optic coefficients in electric-field-poled polymer waveguides. *J. Opt. Soc. Amer. B*, Vol.8, pp. 2311-2317.
- Huang, S.; Kim, T.-D.; Luo, J.; Hau, S. K.; Shi, Z.; Zhou, X.-H.; Yip, H.-L.; Jen, A. K.-Y. (2010) Highly efficient electro-optic polymers through improved poling using a thin TiO₂-modified transparent electrode. *Appl. Phys. Lett.*, Vol.96, pp. 243311.
- Hunziker, C.; Kwon, S.-J.; Figi, H.; Juvalta, F.; Kwon, O.-P.; Jazbinsek, M.; Günter, P. (2008) Configurationally locked, phenolic polyene organic crystal 2-[3-(4-hydroxystyryl)-5,5-dimethylcyclohex-2-enylidene]malononitrile: linear and nonlinear optical properties. *J. Opt. Soc. Am. B*, Vol.25, No.10, pp. 1678-1683.
- Kang, H.; Zhu, P.; Yang, Y.; Faccetti, A.; Marks, T. J. (2004) Self-Assembled Electrooptic Thin Films with Remarkably Blue-Shifted Optical Absorption Based on an X-Shaped Chromophore. *J. Am. Chem. Soc.*, Vol.126, pp. 15974-15975.
- Kim, T.-D.; Luo, J.; Ka, J.-W.; Hau, S.; Tian, Y.; Shi, Z.; Tucker, N. M.; Jang, S.-H.; Kang, J.-W.; Jen, A. K. Y. (2006) Ultralarge and thermally stable electro-optic activities from Diels-Alder crosslinkable polymers containing binary chromophore systems. *Adv. Mater.*, Vol.18, No.22, pp. 3038-3042.
- Kim, T.-D.; Kang, J.-W.; Luo, J.; Jang, S.-H.; Ka, J.-W.; Tucker, N. M.; Benedict, J. B.; Dalton, L. R.; Gray, T.; Overney, R. M.; Park, D. H.; Herman, W. N.; Jen, A. K.-Y. (2007) Ultralarge and Thermally Stable Electro-Optic Activities from Supramolecular Self-Assembled Molecular Glasses. *J. Am. Chem. Soc.*, Vol.129, pp. 488-489.
- Kim, T.-D.; Luo, J.; Cheng, Y.-J.; Shi, Z.; Hau, S.; Jang, S.-H.; Zhou, X. H.; Tian, Y.; Polishak, B.; Huang, S.; Ma, H.; Dalton, L. R.; Jen, A. K.-Y. (2008) Binary Chromophore Systems in Nonlinear Optical Dendrimers and Polymers for Large Electro-Optic Activities. *J. Phys. Chem. C*, Vol.112, No.21, pp. 8091-8098.
- Kim, T.-D.; Luo, J.; Jen, A. K.-Y. (2009) Quantitative determination of the chromophore alignment induced by electrode contact poling in self-assembled NLO materials. *Bull. Korean Chem. Soc.*, Vol.30, No.4, pp. 882-886.
- Kwon, S.-J.; Jazbinsek, M.; Kwon, O.-P.; Gunter, P. (2010) Crystal Growth and Morphology Control of OH1 Organic Electrooptic Crystals. *Cryst. Growth Des.*, Vol.10, pp. 1552-1558.
- Knorr, D. B., Jr. (2010) Molecular Relaxations in Constrained Nanoscale Systems. University of Washington, USA, PhD Dissertation.
- Knorr, D. B., Jr.; Gray, T.; Overney, R. M. (2009) Intrinsic Friction Analysis - Novel Nanoscopic Access to Molecular Mobility in Constrained Organic Systems. *Ultramicroscopy*, Vol.109, No.8, pp. 991.
- Knorr, D. B., Jr.; Zhou, X.-H.; Shi, Z.; Luo, J.; Jang, S.-H.; Jen, A. K.-Y.; Overney, R. M. (2009) Molecular Mobility in Self-Assembled Dendritic Chromophore Glasses. *J. Phys. Chem. B*, Vol.113, No.43, pp. 14180.
- Leahy-Hoppa, M. R.; Cunningham, P. D.; French, J. A.; Hayden, L. M. (2006) Atomistic molecular modeling of the effect of chromophore concentration on the electro-optic coefficient in nonlinear optical polymers. *J. Phys. Chem. A*, Vol.110, pp. 5792-5797.
- Liao, Y.; Anderson, C. A.; Sullivan, P. A.; Akelaitis, A. J. P.; Robinson, B. H.; Dalton, L. R., Electro-Optical Properties of Polymers Containing Alternating Nonlinear Optical Chromophores and Bulky Spacers. *Chem. Mater.* **2006**, Vol.18, No.4, pp. 1062-1067.

- Liu, S.; Haller, M.; Ma, H.; Dalton, L. R.; Jang, S.-H.; Jen, A. K.-Y. (2003) Focused microwave-assisted synthesis of 2,5-dihydrofuran derivatives as electron acceptors for highly efficient nonlinear optical chromophores. *Adv. Mater.*, Vol.15, pp. 603-607.
- McQuarrie, D. A. (2000) *Statistical Mechanics*. University Science Books: Sausalito, CA.
- Michalak, R. J.; Kuo, Y.-H.; Nash, F. D.; Szep, A.; Caffey, J. R.; Payson, P. M.; Haas, F.; McKeon, B. F.; Cook, P. R.; Brost, G. A.; Luo, J.; Jen, A. K.-Y.; Dalton, L. R.; Steier, W. H. (2006) High-speed AJL8/APC polymer modulator. *Photon. Tech. Lett., IEEE*, Vol.18, No.11, pp. 1207-1209.
- Michl, J.; Thulstrup, E. W. (1986) *Spectroscopy with polarized light: solute alignment by photoselection, in liquid crystals, polymers, and membranes*. VCH: Deerfield Beach, FL.
- Munn, R. W.; Ironside, C. N. (1993) *Principles and Applications of Nonlinear Optical Materials*. CRC Press Inc.: Boca Raton, FL.
- Olbricht, B. C.; Sullivan, P. A.; Dennis, P. C.; Hurst, J. T.; Johnson, L. E.; Benight, S. J.; Davies, J. A.; Chen, A.; Eichinger, B. E.; Reid, P. J.; Dalton, L. R.; Robinson, B. H. (2011) Measuring Order in Contact-Poled Organic Electrooptic Materials with Variable-Angle Polarization-Referenced Absorption Spectroscopy (VAPRAS). *J. Phys. Chem. B*, Vol.115, No.2, pp. 231-241.
- Park, D. H.; Lee, C. H.; Herman, W. N. (2006) Analysis of multiple reflection effects in reflective measurements of electro-optic coefficients of poled polymers in multilayer structures. *Optics Express*, Vol.14, No.19, pp. 8866-8884.
- Ponder, J. (2010) *TINKER*, 5.1; Washington University: St. Louis MO.
- Rainbow Photonics AG, (2011) In: *Terahertz Generators and Detectors*, September 28, 2011, Available from: www.rainbowphotonics.com.
- Ray, P. C.; Leszczynski, J. (2004) First hyperpolarizabilities of ionic octupolar molecules: structure-function relationships and solvent effects. *Chem. Phys. Lett.*, Vol.399, pp. 162-166.
- Shi, Y.; Zhang, C.; Zhang, H.; Bechtel, J. H.; Dalton, L. R.; Robinson, B. H.; Steier, W. H. (2000) Low (Sub-1-Volt) Halfwave Voltage Polymeric Electro-Optic Modulators Achieved by Controlling Chromophore Shape. *Science*, Vol.288, pp. 119-122.
- Sprave, M.; Blum, R.; Eich, M. (1996) High electric field conduction mechanisms in electrode poling of electro-optic polymers. *Appl. Phys. Lett.*, Vol.69, No.20, pp. 2962.
- Sills, S.; Gray, T.; Overney, R. (2005) Molecular dissipation phenomena of nanoscopic friction in the heterogeneous relaxation regime of a glass former. *J. Chem. Phys.*, Vol.123, No.13, pp. 134902.
- Starkweather, H. W., Jr. (1981) Simple and complex relaxations. *Macromolecules*, Vol.14, pp. 1277.
- Starkweather, H. W., Jr. (1988) Noncooperative relaxations. *Macromolecules*, Vol.21, No.6, pp. 1798-802.
- Stillinger, F. H. (1977) Axiomatic basis for spaces with noninteger dimension. *Journal of Mathematical Physics*, Vol.18, No.6, pp. 1224-1234.
- Sullivan, P. A.; Rommel, H.; Liao, Y.; Olbricht, B. C.; Akelaitis, A. J. P.; Firestone, K. A.; Kang, J.-W.; Luo, J.; Choi, D. H.; Eichinger, B. E.; Reid, P.; Chen, A.; Robinson, B. H.; Dalton, L. R. (2007) Theory-Guided Design and Synthesis of Multichromophore Dendrimers: An Analysis of the Electro-Optic Effect. *J. Am. Chem. Soc.*, Vol.129, pp. 7523-7530.

- Sun, S.-S.; Dalton, L. R. (2008) *Introduction to Organic Electronic and Optoelectronic Materials and Devices*. CRC Press Taylor and Francis Group: Boca Raton, FL.
- Teng, C. C.; Man, H. T. (1990) Simple reflection technique for measuring the electro-optic coefficient of poling polymers. *Appl. Phys. Lett.*, Vol.56, pp. 1734-1736.
- Tian, Y.; Kong, X.; Nagase, Y.; Iyoda, T. (2003) Photocrosslinkable liquid-crystalline block copolymers with coumarin units synthesized with atom transfer radical polymerization. *J. Polym. Sci., Part A: Polym. Chem.*, Vol.41, pp. 2197-2206.
- Tian, Y.; Akiyama, E.; Nagase, Y.; Kanazawa, A.; Tsutsumi, O.; Ikeda, T. (2004) Synthesis and investigation of photophysical and photochemical properties of new side-group liquid crystalline polymers containing coumarin moieties. *J. Mater. Chem.*, Vol.14, pp. 3524-3531.
- Valore, A.; Cariati, E.; Righetto, S.; Roberto, D.; Tessore, F.; Ugo, R.; Fragala, I. L.; Fragala, M. E.; Malandrino, G.; De Angelis, F.; Belpassi, L.; Ledoux-Rak, I.; Hoang Thi, K.; Zyss, J. (2010) Fluorinated -Diketonate Diglyme Lanthanide Complexes as New Second-Order Nonlinear Optical Chromophores: The Role of f Electrons in the Dipolar and Octupolar Contribution to Quadratic Hyperpolarizability. *J. Am. Chem. Soc.*, Vol.132, pp. 4966-4970.
- van der Boom, M. E.; Richter, A. G.; Malinsky, J. E.; Lee, P. A.; Armstrong, N. R.; Dutta, P.; Marks, T. J. (2001) Single Reactor Route to Polar Superlattices. Layer-by-Layer Self-Assembly of Large-Response Molecular Electrooptic Materials by Protection-Deprotection. *Chem. Mater.*, Vol.13, pp. 15-17.
- Verbiest, T.; Clays, K.; Rodriguez, V. (2009) *Second-order Nonlinear Optical Characterization Techniques: an Introduction*. CRC Press: Taylor and Francis Group: Boca Raton, FL.
- Wang, Z.; Sun, W.; Chen, A.; Kosilkin, I.; Bale, D.; Dalton, L. R. (2011) Organic electro-optic thin films by simultaneous vacuum deposition and laser-assisted poling. *Opt. Lett.*, Vol.36, No.15, pp. 2853-2855.
- Ward, I. M. (1971) *Mechanical Properties of Solid Polymers*. Wiley-Interscience: London.
- Weder, C.; Glomm, B. H.; Neuenschwander, P.; Suter, U. W.; Pretre, P.; Kaatz, P.; Gunter, P. (1997) New polyamide main-chain polymers based on 2',5'-diamino-4-(dimethylamino)-4'-nitrostilbene (DDANS). *Adv. Nonlinear Opt.*, Vol.4, pp. 63-76.
- Williams, M. L.; Landel, R. E.; Ferry, F. D. (1995) The Temperature Dependence of Relaxation Mechanisms in Amorphous Polymers and Other Glass-forming Liquids. *J. Am. Chem. Soc.*, Vol.77, pp. 3701.
- Woollam, J. A. (2000) Ellipsometry, Variable Angle Spectroscopic. In *Wiley Encyclopedia of Electrical and Electronics Engineering*, Wiley: New York, pp 109-117.
- Yang, Z.; Worle, M.; Mutter, L.; Jazbinsek, M.; Gunter, P. (2007) Synthesis, Crystal Structure, and Second-Order Nonlinear Optical Properties of New Stilbazolium Salts. *Cryst. Growth. and Design*, Vol.7, No.1, pp. 83-86.
- Zhang, C.; Dalton, L. R.; Oh, M. C.; Zhang, H.; Steier, W. H. (2001) Low V(π) Electrooptic Modulators from CLD-1: Chromophore Design and Synthesis, Material Processing, and Characterization. *Chem. Mater.*, Vol.13, No.9, pp. 3043-3050.
- Zhou, X. H.; Luo, J.; Huang, S.; Kim, T. D.; Shi, Z.; Cheng, Y.-J.; Jang, S.-H.; Knorr, D. B., Jr.; Overney, R. M.; Jen, A. K.-Y. (2009) Supramolecular Self-Assembled Dendritic Nonlinear Optical Chromophores: Fine-Tuning of Arene-Perfluoroarene Interactions for Ultralarge Electro-Optic Activity and Enhanced Thermal Stability. *Adv. Mater.* Vol.21, No.19, pp. 1976.



Molecular Interactions

Edited by Prof. Aurelia Meghea

ISBN 978-953-51-0079-9

Hard cover, 400 pages

Publisher InTech

Published online 29, February, 2012

Published in print edition February, 2012

In a classical approach materials science is mainly dealing with interatomic interactions within molecules, without paying much interest on weak intermolecular interactions. However, the variety of structures actually is the result of weak ordering because of noncovalent interactions. Indeed, for self-assembly to be possible in soft materials, it is evident that forces between molecules must be much weaker than covalent bonds between the atoms of a molecule. The weak intermolecular interactions responsible for molecular ordering in soft materials include hydrogen bonds, coordination bonds in ligands and complexes, ionic and dipolar interactions, van der Waals forces, and hydrophobic interactions. Recent evolutions in nanosciences and nanotechnologies provide strong arguments to support the opportunity and importance of the topics approached in this book, the fundamental and applicative aspects related to molecular interactions being of large interest in both research and innovative environments. We expect this book to have a strong impact at various education and research training levels, for young and experienced researchers from both academia and industry.

How to reference

In order to correctly reference this scholarly work, feel free to copy and paste the following:

Stephanie J. Benight, Bruce H. Robinson and Larry R. Dalton (2012). Nano-Engineering of Molecular Interactions in Organic Electro-Optic Materials, *Molecular Interactions*, Prof. Aurelia Meghea (Ed.), ISBN: 978-953-51-0079-9, InTech, Available from: <http://www.intechopen.com/books/molecular-interactions/nano-engineering-of-molecular-interactions-in-organic-electro-optic-materials>

INTECH

open science | open minds

InTech Europe

University Campus STeP Ri

Slavka Krautzeka 83/A

51000 Rijeka, Croatia

Phone: +385 (51) 770 447

Fax: +385 (51) 686 166

www.intechopen.com

InTech China

Unit 405, Office Block, Hotel Equatorial Shanghai

No.65, Yan An Road (West), Shanghai, 200040, China

中国上海市延安西路65号上海国际贵都大饭店办公楼405单元

Phone: +86-21-62489820

Fax: +86-21-62489821

© 2012 The Author(s). Licensee IntechOpen. This is an open access article distributed under the terms of the [Creative Commons Attribution 3.0 License](#), which permits unrestricted use, distribution, and reproduction in any medium, provided the original work is properly cited.